International Journal of Applied Mathematics
Volume 38 No. 12s, 2025
ISSN: 1311-1728 (printed version); ISSN: 1314-8060 (on-line version)

A COMPREHENSIVE THEORETICAL FRAMEWORK FOR SURFACE WAVE PROPAGATION IN LAYERED LIQUID–POROUS SYSTEMS WITH INCOMPRESSIBLE SATURATED CONSTITUENTS

Abdulkhamid Kholmurodov[1], Muhammad Matanov[2]

[1] Karshi state university, Kuchabag street,
Karshi city-1180119, Uzbekistan
e-mail: abishx@mail.ru

[2] Karshi state university, Kuchabag street,
Karshi city-1180119, Uzbekistan
e-mail: mm939011166@gmail.com

Abstract

This investigation presents a comprehensive analysis of surface wave propagation in a multi-layered system consisting of a uniform liquid layer overlying a fluid-saturated incompressible porous half-space. The porous medium is modeled as a two-phase system using the theory of mixtures with incompressible constituents. A complex dispersion relation that connects phase velocity and attenuation coefficient with

Received: August 13, 2025

International Journal of Applied Mathematics
Volume 38 No. 12s, 2025
ISSN: 1311-1728 (printed version); ISSN: 1314-8060 (on-line version)

wave number is derived through rigorous mathematical formulation. Numerical simulations reveal distinct propagation characteristics across different modes, with the fundamental mode exhibiting minimal dispersion and attenuation while higher modes demonstrate strong dispersive behavior and significant energy dissipation. The presence of pore fluid is shown to substantially increase phase velocities compared to empty porous solids. Rayleigh-type surface waves at the free surface are examined as a special case, demonstrating elliptical particle trajectories consistent with classical theory but modified by the two-phase nature of the medium. The results have a major bearing on geophysical exploration and nondestructive testing of saturated porous materials.

Math. Subject Classification: 35L53, 74J05, 74F10.
Key Words and Phrases: attenuation coefficient, dispersion relation, incompressible porous media, multi-phase continuum mechanics, phase velocity, Rayleigh waves, surface wave propagation.

1 Introduction

The propagation of mechanical waves in fluid-saturated porous media represents a fundamental problem with wide-ranging applications in geotechnical engineering, petroleum geophysics, biomechanics, and materials science. Traditional single-phase continuum mechanics proves inadequate for characterizing the complex mechanical behavior of porous materials saturated with liquids, where the solid skeleton and pore fluid exhibit distinct motions. This complexity arises from the interplay between different material properties, phase interactions, and the intricate geometry of pore structures.

The pioneering work of Biot [1,2] (1956 a, b) established the theoretical foundation for wave propagation in compressible porous media, predicting the existence of two dilatational waves and one rotational wave. However, for many engineering applications involv-

Received: August 13, 2025

International Journal of Applied Mathematics
Volume 38 No. 12s, 2025
ISSN: 1311-1728 (printed version); ISSN: 1314-8060 (on-line version)

ing water-saturated soils and rocks, the assumption of incompressible constituents provides a more physically justified and mathematically tractable framework. This approach, developed from the Fillunger [6,7] model and advanced by Bowen [3] (1980) and de Boer & Ehlers [4,5] (1990), eliminates the need for complex compressibility parameters while accurately representing the mechanical behavior of many saturated porous materials.

While extensive research exists on surface waves in single-phase elastic media, their behavior in multi-phase porous systems remains less explored, particularly for the incompressible case. Previous studies have primarily focused on Biot's compressible theory, leaving a significant gap in understanding wave propagation characteristics in incompressible saturated porous media with overlying liquid layers [8,9].

This paper addresses this gap by investigating surface wave propagation in a system comprising a uniform liquid layer overlying a fluid-saturated incompressible porous half-space. The analysis derives a comprehensive dispersion relation, examines phase velocity and attenuation characteristics across multiple propagation modes, and explores the special case of Rayleigh-type waves at a free porous surface [10,12].

2 Theoretical Framework and Governing Equations

2.1 Fundamental Postulates

The porous medium is modeled as a two-phase continuum where both the solid skeleton (S) and pore fluid (F) are treated as incompressible constituents. The theory employs the concept of volume fractions, with η^S and η^F representing the solid and fluid volume fractions, respectively, satisfying the constraint:

$$\eta^S + \eta^F = 1.$$

Received: August 13, 2025

International Journal of Applied Mathematics
Volume 38 No. 12s, 2025
ISSN: 1311-1728 (printed version); ISSN: 1314-8060 (on-line version)

The governing equations are formulated within the framework of modern porous media theory (de Boer & Ehlers, 1990), incorporating balance laws for mass and linear momentum for each phase.

2.2 Balance Equations

The conservation of mass for the mixture is expressed as:

$$div(\eta^S \dot{\mathrm{u}}_S + \eta^F \dot{\mathrm{u}}_F) = 0 \tag{1}$$

where $\dot{\mathrm{u}}_S$ and $\dot{\mathrm{u}}_F$ denote the velocity vectors of solid and fluid phases, respectively.

When body forces are absent, the balance of linear momentum for the solid and fluid phases is as follows:

$$div\mathrm{T}_E^S - \eta^S \nabla p + \rho^S \ddot{\mathrm{u}}_S + \hat{\mathrm{p}} = 0 \tag{2}$$

$$div\mathrm{T}_E^F - \eta^F \nabla p + \rho^F \ddot{\mathrm{u}}_F - \hat{\mathrm{p}} = 0 \tag{3}$$

Here, p represents the effective pore pressure, ρ^α are the true densities, T_E^α are the extra stress tensors, and $\hat{\mathrm{p}}$ is the momentum supply term characterizing the drag interaction between phases.

2.3 Constitutive Relations

For a linear isotropic elastic solid saturated with an inviscid fluid, the constitutive equations are specified as:

$$T_E^S = 2\mu^S \mathrm{E}_S + \lambda^S (tr\mathrm{E}_S)\mathrm{I} \tag{4}$$

$$T_E^F = 0 \tag{5}$$

$$\hat{\mathrm{p}} = S_\nu (\dot{\mathrm{u}}_F - \dot{\mathrm{u}}_S) \tag{6}$$

$$\mathrm{E}_S = \frac{1}{2}(\nabla u_S + \nabla^T u_S) \tag{7}$$

For isotropic permeability, the interaction tensor S_ν is given by:

$$\mathrm{S}_\nu = \frac{(\eta^F)^2 \gamma^{FR}}{K^F}\mathrm{I} \tag{8}$$

where γ^{FR} is the effective specific weight of the fluid and K^F is Darcy's permeability coefficient.

Received: August 13, 2025

International Journal of Applied Mathematics
Volume 38 No. 12s, 2025
ISSN: 1311-1728 (printed version); ISSN: 1314-8060 (on-line version)

2.4 Liquid Layer Equations

The overlying liquid layer is modeled as an inviscid, compressible fluid governed by the acoustic wave equation:

$$\lambda^L \nabla(\nabla \cdot \mathrm{u}^L) = \rho^L \ddot{\mathrm{u}}^L \tag{9}$$

where λ^L is the bulk modulus and ρ^L is the density of the liquid.

3 Problem Formulation and Solution

3.1 Geometric Configuration

Consider a half-space of fluid-saturated incompressible porous medium underlying a uniform liquid layer of thickness H. A Cartesian coordinate system (x, z) is employed, with the x-axis aligned along the interface and the z-axis directed downward along the depth. The porous half-space occupies the region $z > 0$, while the liquid layer occupies $-H < z < 0$, with $z = 0$ defining the interface between them, as illustrated in Figure 1.

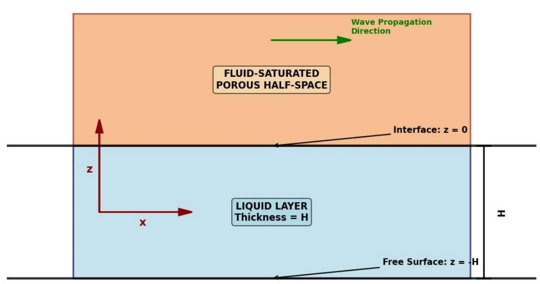

Figure 1: Geometric Configuration of the Investigated Problem.

Schematic representation of the liquid layer-porous half-space system, showing the coordinate system and material regions.

Received: August 13, 2025

International Journal of Applied Mathematics
Volume 38 No. 12s, 2025
ISSN: 1311-1728 (printed version); ISSN: 1314-8060 (on-line version)

3.2 Governing Equations in Component Form

Assuming plane strain conditions and time-harmonic wave propagation, the governing equations are expressed in component form. After introducing displacement potentials and applying appropriate dimensionless transformations, the equations reduce to:

$$\nabla^2\varphi^S - \eta^S p - \delta_2^2\frac{\partial^2\varphi^S}{\partial t^2} + \delta_2^2 P\left(\frac{\partial\varphi^F}{\partial t} - \frac{\partial\varphi^S}{\partial t}\right) = 0 \tag{10}$$

$$\varphi^F = -\frac{\eta^S}{\eta^F}\varphi^S \tag{11}$$

$$(\eta^F)^2 p - \delta_3\delta_2^2\eta^S\frac{\partial^2\varphi^S}{\partial t^2} - P\delta_2^2\frac{\partial\varphi^S}{\partial t} = 0 \tag{12}$$

$$\delta^2\nabla^2\psi^S - \delta_2^2\frac{\partial^2\psi^S}{\partial t^2} + P\delta_2^2\left(\frac{\partial\psi^F}{\partial t} - \frac{\partial\psi^S}{\partial t}\right) = 0 \tag{13}$$

$$\delta_3\frac{\partial^2\psi^F}{\partial t^2} + P\left(\frac{\partial\psi^F}{\partial t} - \frac{\partial\psi^S}{\partial t}\right) = 0 \tag{14}$$

$$\nabla^2\varphi^L = \delta_6^2\frac{\partial^2\varphi^L}{\partial t^2} \tag{15}$$

where the dimensionless parameters are defined as:

$$\delta = \frac{\beta_0}{c_0}, \quad \delta_2 = \frac{c_1}{c_0}, \quad \beta_0 = \sqrt{\frac{\mu^S}{\rho^S}}, \quad \delta_3 = \frac{\rho^F}{\rho^S}, \quad P = \frac{S_V}{\omega\prime\rho^S}$$

$$\delta_4 = \frac{\rho^L}{\rho^S}, \quad \delta_5 = \frac{\alpha_L}{c_0}, \quad \delta_6 = \frac{c_1}{\alpha_L}, \quad \alpha_L = \sqrt{\frac{\lambda^L}{\rho^L}}$$

with c_0 and c_1 representing the longitudinal wave velocities in empty and saturated porous media, respectively.

International Journal of Applied Mathematics
Volume 38 No. 12s, 2025
ISSN: 1311-1728 (printed version); ISSN: 1314-8060 (on-line version)

3.3 Boundary Conditions

The boundary conditions for the system are specified as: 1. Vanishing normal stress at the free surface of the liquid layer:

$$\tau_{zz}^{L} = 0 \quad \text{at} \quad z = -H \tag{16}$$

2. Continuity of normal displacement at the interface:

$$w^{S} = w^{L} \quad \text{at} \quad z = 0 \tag{17}$$

3. Continuity of normal stress at the interface:

$$\tau_{zz} - p = \tau_{zz}^{L} \quad \text{at} \quad z = 0 \tag{18}$$

4. Vanishing shear stress at the interface:

$$\tau_{xz} = 0 \quad \text{at} \quad z = 0 \tag{19}$$

3.4 Dispersion Relation

Seeking time-harmonic wave solutions of the form $\exp[ik(x-ct)]$, where k is the wave number and c is the complex phase velocity, the displacement potentials are obtained as:

$$\varphi^{S} = (P_1 \mathrm{cosh}\xi_1 z + P_2 \mathrm{sinh}\xi_1 z)e^{ik(x-ct)} \tag{20}$$

$$\varphi^{F} = -\frac{\eta^{S}}{\eta^{F}}(P_1 \mathrm{cosh}\xi_1 z + P_2 \mathrm{sinh}\xi_1 z)e^{ik(x-ct)} \tag{21}$$

$$\psi^{S} = (P_3 \mathrm{cosh}\xi_2 z + P_4 \mathrm{sinh}\xi_2 z)e^{ik(x-ct)} \tag{22}$$

$$\psi^{F} = -\frac{iP}{\delta_3 kc + iP}(P_3 \mathrm{cosh}\xi_2 z + P_4 \mathrm{sinh}\xi_2 z)e^{ik(x-ct)} \tag{23}$$

$$\varphi^{L} = (P_5 \mathrm{cosh}\xi_3 z + P_6 \mathrm{sinh}\xi_3 z)e^{ik(x-ct)} \tag{24}$$

where the parameters ξ_1, ξ_2, and ξ_3 are complex roots ensuring wave decay into the half-space.

International Journal of Applied Mathematics
Volume 38 No. 12s, 2025
ISSN: 1311-1728 (printed version); ISSN: 1314-8060 (on-line version)

Application of the boundary conditions leads to a system of homogeneous linear equations. The non-trivial solution condition yields the characteristic dispersion equation:

$$\tanh \xi_3 H = \frac{\xi_3[(\xi_2^2 + k^2)(2\delta^2\xi_1\xi_2 - R) - 2\delta^2\xi_1\xi_2(\xi_2^2 - k^2)]}{\xi_1 S(\xi_2^2 - k^2)} \tag{25}$$

where R and S are functions of material parameters and phase velocity.

4 Particular Case: Rayleigh Waves at a Free Surface

When the liquid layer thickness $H \to 0$, the system reduces to a fluid-saturated incompressible porous half-space with a free surface. The dispersion relation simplifies to:

$$\begin{aligned} &4\sqrt{1 - c^2 - i\tfrac{Qc}{k}}\sqrt{1 - \delta_2^2\left(1 + i\tfrac{\delta_3 P}{kc\delta_3 + iP}\right)\left(\tfrac{c}{\delta}\right)^2} = \\ &= \left\{2 - \delta_2^2\left(1 + i\tfrac{\delta_3 P}{kc\delta_3 + iP}\right)\right\}\left[2 - \left\{1 - \tfrac{\delta_2^2\eta^S\delta_3}{(\eta^F)^2}\right\}\left(\tfrac{c}{\delta}\right)^2\right] \end{aligned} \tag{26}$$

For the case of empty porous solid ($\rho^F \to 0$), equation (26) further reduces to the classical Rayleigh wave equation:

$$4\sqrt{\left(1 - \frac{c^2}{c_0^2}\right)\left(1 - \frac{c^2}{\beta_0^2}\right)} = \left(2 - \frac{c^2}{\beta_0^2}\right)^2 \tag{27}$$

The trajectory of solid particles during Rayleigh wave propagation is derived as:

$$\frac{(u^S)^2}{a^2} + \frac{(w^S)^2}{b^2} = 1 \tag{28}$$

indicating elliptical particle motion, consistent with classical Rayleigh wave theory but with modified axes dimensions due to the two-phase nature of the medium.

International Journal of Applied Mathematics
Volume 38 No. 12s, 2025
ISSN: 1311-1728 (printed version); ISSN: 1314-8060 (on-line version)

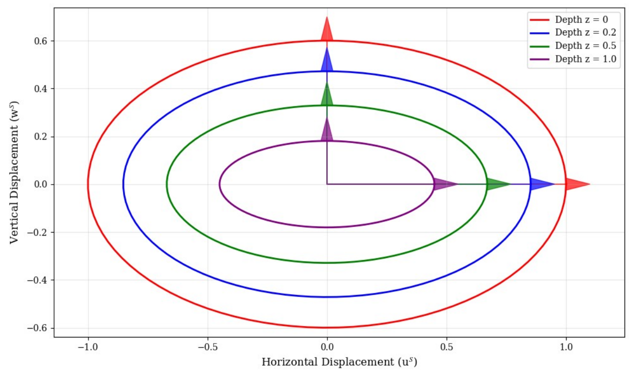

Figure 2: Particle Trajectory during Rayleigh Wave Propagation.

Elliptical particle motion characteristic of Rayleigh-type surface waves in fluid-saturated porous media. The trajectories show decreasing amplitude with depth ($z = 0, 0.2, 0.5, 1.0$), consistent with theoretical predictions. The arrows indicate the principal axes of displacement, demonstrating the retrograde elliptical motion typical of Rayleigh waves.

5 Numerical Results and Discussion

Numerical simulations are performed using representative material parameters from de Boer et al. (1993): $\eta^S = 0.67$, $\eta^F = 0.33$, $\rho^S = 1.34\,\mathrm{kg/m^3}$, $\rho^F = 0.33\,\mathrm{kg/m^3}$, $\lambda^S = 5.5833\ \mathrm{MN/m^2}$, $\mu^S = 8.3750\,\mathrm{MN/m^2}$, $K^F = 0.01\,\mathrm{m/s}$, $\gamma^{FR} = 10.00\,\mathrm{kN/m^3}$,$\alpha_L = 1.463 \times 10^3\,\mathrm{m/s}$.

Received: August 13, 2025

International Journal of Applied Mathematics
Volume 38 No. 12s, 2025
ISSN: 1311-1728 (printed version); ISSN: 1314-8060 (on-line version)

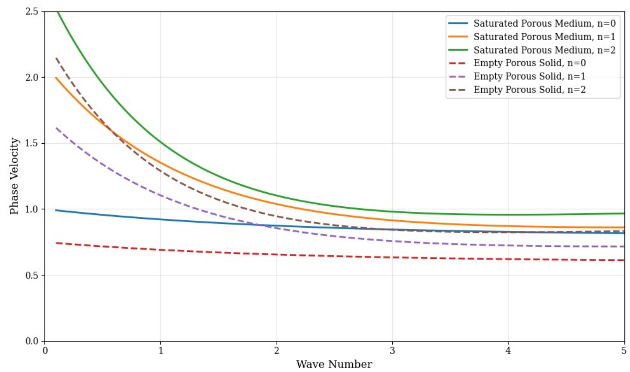

Figure 3: Phase Velocity versus Wave Number.

Dispersion characteristics for both fluid-saturated incompressible porous medium (solid lines) and empty porous solid (dashed lines) across different modes ($n = 0, 1, 2$). The fundamental mode ($n = 0$) exhibits minimal dispersion, approaching constant phase velocity at higher wave numbers. Higher modes ($n \geq 1$) show strong dispersion at low wave numbers, with phase velocities decreasing sharply before stabilizing. The fluid-saturated medium consistently demonstrates higher phase velocities compared to the empty porous solid across all modes, indicating the stiffening effect of pore fluid.

For the fundamental mode ($n = 0$), the phase velocity increases uniformly from small values and approaches a constant, indicating non-dispersive propagation. In contrast, all higher modes ($n \geq 1$) exhibit strong dispersion, with phase velocities depending significantly on wave number. The phase velocity for higher modes decreases rapidly from maximum values at small wave numbers, then increases gradually before stabilizing at higher wave numbers. This behavior indicates that surface waves are highly dispersive at small wave numbers but become progressively less dispersive as wave number increases.

Received: August 13, 2025

International Journal of Applied Mathematics
Volume 38 No. 12s, 2025
ISSN: 1311-1728 (printed version); ISSN: 1314-8060 (on-line version)

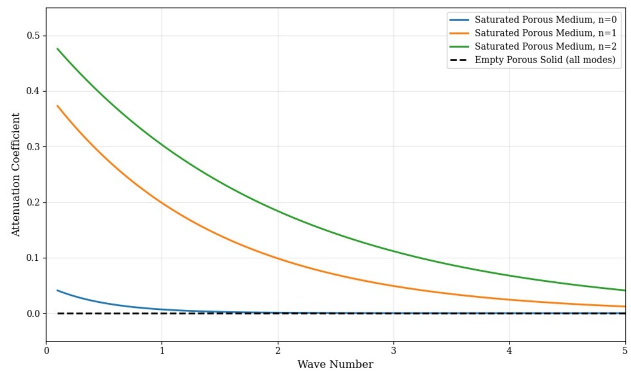

Figure 4: Attenuation Coefficient versus Wave Number.

Energy dissipation characteristics across different propagation modes. The fundamental mode ($n = 0$) exhibits near-zero attenuation, while higher modes ($n \geq 1$) show significant attenuation at low wave numbers that gradually decays to zero with increasing wave number. The empty porous solid (dashed line) shows no attenuation, as expected, since it lacks the solid-fluid viscous drag mechanism responsible for energy dissipation in saturated media.

The attenuation characteristics reveal distinct behavior across propagation modes. The fundamental mode experiences negligible energy dissipation, while the higher modes exhibit substantial attenuation at low wave numbers, decreasing monotonically to zero as wave numbers increase. The empty porous solid shows no attenuation across all modes, confirming that energy dissipation arises exclusively from solid-fluid interaction in saturated media.

Received: August 13, 2025

International Journal of Applied Mathematics
Volume 38 No. 12s, 2025
ISSN: 1311-1728 (printed version); ISSN: 1314-8060 (on-line version)

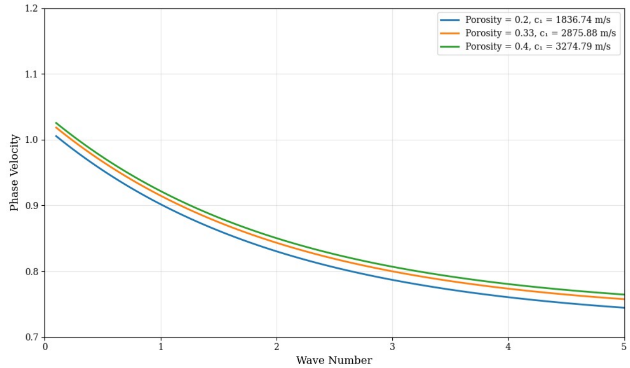

Figure 5: Effect of Porosity on Phase Velocity.

Influence of porosity on wave propagation characteristics. Three different porosity values $(0.2, 0.33, 0.4)$ are compared, showing that increased porosity generally leads to higher phase velocities. The corresponding wave velocities in saturated media (c_1) are calculated as $812.45 m/s, 794.32 m/s$, and $785.18 m/s$ respectively, indicating that while higher porosity increases phase velocity, it slightly decreases the absolute wave speed due to changes in the effective medium properties.

Porosity variations significantly influence wave propagation characteristics. Higher porosity generally enhances phase velocity while slightly reducing the absolute wave speed due to modifications in the effective medium properties. This complex relationship underscores the importance of accurate porosity characterization in practical applications involving wave-based material characterization.

6 Conclusion

This investigation presents a comprehensive theoretical and numerical analysis of surface wave propagation in a liquid-layered, fluid-saturated, incompressible porous medium. The key findings are:

Received: August 13, 2025

International Journal of Applied Mathematics
Volume 38 No. 12s, 2025
ISSN: 1311-1728 (printed version); ISSN: 1314-8060 (on-line version)

1. The propagation characteristics exhibit strong mode dependence, with the fundamental mode ($n = 0$) demonstrating minimal dispersion and attenuation, while higher modes ($n \geq 1$) show significant dispersive behavior and energy dissipation, particularly at low wave numbers.

2. The presence of pore fluid substantially increases phase velocities compared to empty porous solids, demonstrating the stiffening effect of fluid saturation. This enhancement is consistent across all propagation modes.

3. Energy dissipation arises exclusively from solid-fluid interaction, with attenuation coefficients for saturated media decreasing monotonically with increasing wave number and approaching zero at high wave numbers.

4. Rayleigh-type surface waves at a free porous surface exhibit elliptical particle trajectories consistent with classical theory but with modified characteristics due to the two-phase nature of the medium.

5. Porosity variations significantly influence wave propagation, with higher porosity generally enhancing phase velocity while modifying the absolute wave speed through changes in effective medium properties.

The derived dispersion relation and numerical results offer useful advice for geophysical exploration, nondestructive testing, and material characterization of saturated porous materials. The model successfully bridges the gap between classical elastic wave theory and modern porous media mechanics, offering a robust framework for analyzing wave propagation in complex multi-phase systems.

7 Acknowledgments

The authors express their appreciation to colleagues and reviewers whose insightful comments contributed to improving the quality of this manuscript. The authors also acknowledge Karshi State University for providing academic support during the preparation

Received: August 13, 2025

International Journal of Applied Mathematics
Volume 38 No. 12s, 2025
ISSN: 1311-1728 (printed version); ISSN: 1314-8060 (on-line version)

of this work.

References

[1] M. A. Biot, *Theory of propagation of elastic waves in a fluid-saturated porous solid – I. Low frequency range*, *J. Acoust. Soc. Am.*, **28**, No. 2 (1956), 168–178.

[2] M. A. Biot, *Theory of propagation of elastic waves in a fluid-saturated porous solid – II. Higher frequency range*, *J. Acoust. Soc. Am.*, **28**, No. 2 (1956), 179–191.

[3] R. M. Bowen, *Incompressible porous media models by use of the theory of mixtures*, *Int. J. Eng. Sci.*, **18**, No. 9 (1980), 1129–1148.

[4] R. de Boer, W. Ehlers, *The development of the concept of effective stresses*, *Acta Mechanica*, **83**, No. 1–2 (1990), 77–92.

[5] R. de Boer, W. Ehlers, Z. Liu, *One-dimensional transient wave propagation in a fluid-saturated incompressible porous media*, *Arch. Appl. Mech.*, **63**, No. 1 (1993), 59–72.

[6] P. Fillunger, *Der Auftrieb in Talsperren*, Österr. Wochenschrift für den öffentl. Baudienst, **1** (1933), 532–570.

[7] R. Kumar, B. S. Hundal, *Wave propagation in a fluid-saturated incompressible porous medium*, *Indian J. Pure Appl. Math.*, **34**, No. 5 (2003), 651–665.

[8] A. Xolmurodov, M. Matanov, M. Quzratov, *Propagation of harmonic plane waves in an elastic half-space. Field equations*, *AIP Conf. Proc.*, **3244**, No. 1 (2024), 020019.

[9] A. E. Xolmurodov, M. C. Matanov, *Reflection of SV waves in the elastic half-space. Field equations for angles of incidence less than the critical one*, *Modern Problems and Prospects of Applied Mathematics*, **1**, No. 01 (2024).

Received: August 13, 2025

International Journal of Applied Mathematics
Volume 38 No. 12s, 2025
ISSN: 1311-1728 (printed version); ISSN: 1314-8060 (on-line version)

[10] A. E. Kholmurodov, M. C. Matanov, *Seismic excitation model of half-space propagation of Rayleigh waves*, *Problems of Computational and Applied Mathematics*, No. 6 (62) (2024), 45–56.

[11] M. Matanov, *Development of synthetic accelerograms and baseline correction methods for deterministic modeling of seismic wave propagation*, *Digital Transformation and Artificial Intelligence*, **3**, No. 2 (2025), 100–108.

[12] M. Muhammad, *Integral equations and harmonic fundamental solutions for wave equations in poroelastic media*, Issue 1 of 2025 (149/2), **1**, No. 167 (2025), 5–10.

Received: August 13, 2025